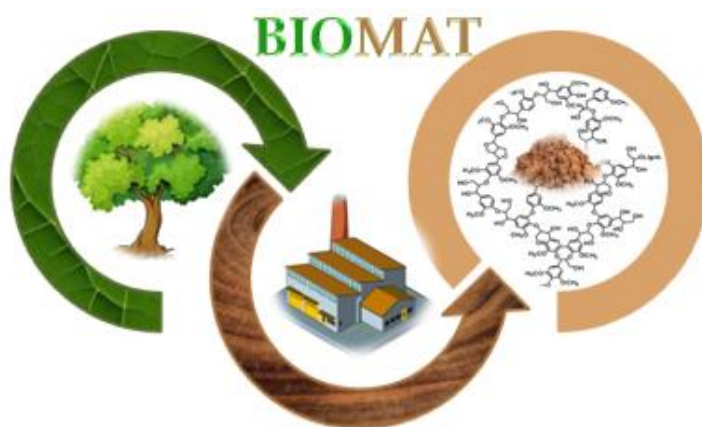


Ss. CYRIL AND METHODIUS UNIVERSITY IN SKOPJE, MACEDONIA



Part 3

Green composites obtained with valorization of wood lignin, and their characterization

authors:

JADRANKA BLAZHEVSKA GILEV, MARIJA PROSHEVA, ANDREA PETANOVA

Skopje 2025

The e-script was created as part of the project titled

*“Improving teaching competencies in design of new generation biomaterials
from wood waste”*

Project reference: 2024-1-PL01-KA220-HED-000246133

from the Erasmus+ programme:

KA220-HED - Cooperation partnerships in higher education.

1. Laser ablation

Introduction

Laser is an abbreviation that stands for Light Amplification by Stimulated Emission of Radiation (LASER). Lasers are characterized by monochromaticity, i.e. a beam with a single wavelength is generated, coherence, all photons have the same polarization and collimation, i.e. the laser beam is not dispersed and can be focused into a point with a small diameter (Claverie, 2020). The term ablation refers to the removal of material through melting or evaporation caused by the absorption of energy, such as from electrical discharges or a laser beam. Laser ablation uses laser energy to remove material through melting, sublimation, ionization, erosion, or explosion, forming vapor, plasma, or fine particles. Laser ablation can be a thermal or non-thermal process for removing atoms from solids using a continuous wave (CW) or pulsed laser. Continuous beam lasers emit a continuous beam, while pulsed lasers emit a beam of short duration (Russo et al., 2007; Zhang and Guan, 2014).

When a solid surface is irradiated with a continuous or pulsed laser, the material begins to heat up due to absorption of laser energy. As a result, the thermal motion of some particles is accelerated. Once the absorbed energy exceeds the sublimation energy, these particles of the solid material begin to evaporate or sublime, i.e. a cloud of "vapor" forms above the material, i.e. part of the material is ablated. The laser ablation rate \dot{N} is defined as the particles ablated per unit area per second, formula 1.

$$\dot{N} = \rho d / \tau m \quad (1)$$

Where, τ is the duration of the laser pulse, ρ represents the density of the target, d is the thickness of the ablated material and m is the mass of the ablated atoms (D. Zhang and Guan, 2014).

Depending on the duration of the laser beam and the interactions between the laser photons and the material, laser ablation mechanisms can be divided into two groups:

- Thermal ablation – the material absorbs the laser energy and converts it into heat, as a result of which the material begins to evaporate. This mechanism depends on the thermal characteristics of the material (thermal conductivity and melting point). Thermal ablation mainly occurs when ablating with longer laser pulses (Ravi-Kumar et al., 2019).
- Photochemical ablation – occurs when the energy of the laser beam is high enough to cause direct breaking of chemical bonds in the material without a significant increase in temperature. As a result, the material being ablated suffers negligible thermal damage. Photochemical ablation is characteristic of ultraviolet lasers that have high photon energy (Ravi-Kumar et al., 2019).

Pulsed laser ablation is a commonly used technique for depositing thin films, the deposition using a laser is called pulsed laser deposition and takes place in several steps:

- 1) Laser ablation and plasma formation: A high-energy pulsed laser beam is focused onto the surface of the target (the material being ablated), causing rapid energy absorption and heating of the surface to the point of vaporization. This leads to vaporization and ionization of the target material, forming high-density plasma at the surface.

- 2) Isothermal and adiabatic expansion of the plasma: The formed plasma cloud continues to absorb energy from the laser, which leads to an increase in temperature and internal pressure. As a result, the plasma expands perpendicular to the target surface, forming an elliptical cloud.
- 3) Thin film deposition: The plasma moves through the reactor and when it reaches the substrate surface, the gaseous particles combine and aggregate, forming a thin film on the substrate surface (D. Zhang and Guan, 2014).

Figure 1.1. shows the process of depositing a thin film by pulsed laser ablation/deposition.

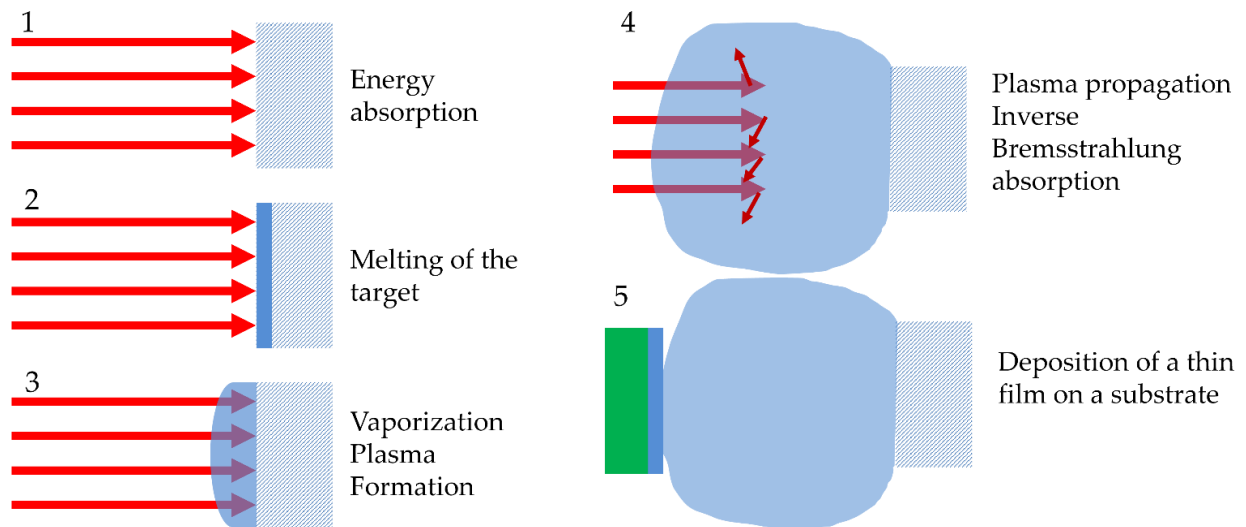


Figure 1.1. Schematic representation of the thin film deposition process by pulsed laser ablation/deposition.

The characteristics of the laser beam, such as: pulse duration, wavelength, pulse frequency, energy density, focus position, and scanning mode, have a major impact on the ablation process. Shorter pulses allow for a greater degree of vaporization with minimal melting, while longer pulses cause more thermal diffusion and greater thermal damage. For greater ablation efficiency and to avoid large thermal damage, the wavelength of the laser beam should be matched to the optical properties of the material. That is, different materials absorb rays of different wavelengths. The pulse repetition rate is also of great importance, the optimal pulse repetition rate prevents heat buildup and allows the plasma cloud to disperse between two pulses. The energy density must be above the ablation threshold of the material for successful particle separation. Additionally, the laser beam needs to be properly focused in order to concentrate the energy on the target, which allows for successful ablation of the material and the formation of a plasma that is then deposited on a suitable substrate (Ravi-Kumar et al., 2019).

Due to its relative simplicity, speed, and ability for precise control, laser ablation/deposition has wide applications in industry, science, and technology for the production of high-quality films and structures.

Experimental part

Purpose of the experiment

Thin film deposition via laser ablation of lignin.

Equipment

Pulsed Infrared TEA (Transversely Excited Atmospheric) CO₂ Laser

Hydraulic Press

Turbomolecular Pump

Chemicals

Lignin

Procedure

Before starting the thin film deposition, the lignin was pressed into a compact tablet (target) using a hydraulic press. The thin film deposition was performed in a glass reactor closed with a NaCl lens. The target and the corresponding substrates on which the film was applied were placed at a distance of about 45 mm. A vacuum of 10^{-3} Pa was achieved using a turbomolecular pump. To achieve uniform film deposition, as well as to optimize material properties, the holders on which the target and substrates were placed were manually rotated during the experiment. The laser beam was focused on the target surface through a ZnSe lens ($F=500$ mm) mounted on a diaphragm with an aperture of 25 cm. The beam intensity was 15 J/m^2 . The pulse frequency was 1 Hz; the duration of the experiment was 80 minutes. Copper plates, glass and corundum were used as substrates in order for the deposited film to be successfully analyzed by various spectroscopic techniques.

Figure 1.2 shows a schematic representation of the process of deposition of thin films by laser ablation.

Interpretation of results

- To investigate the optical properties using UV-Vis spectroscopy.
- To study the morphology of the resulting thin film using scanning electron microscopy.

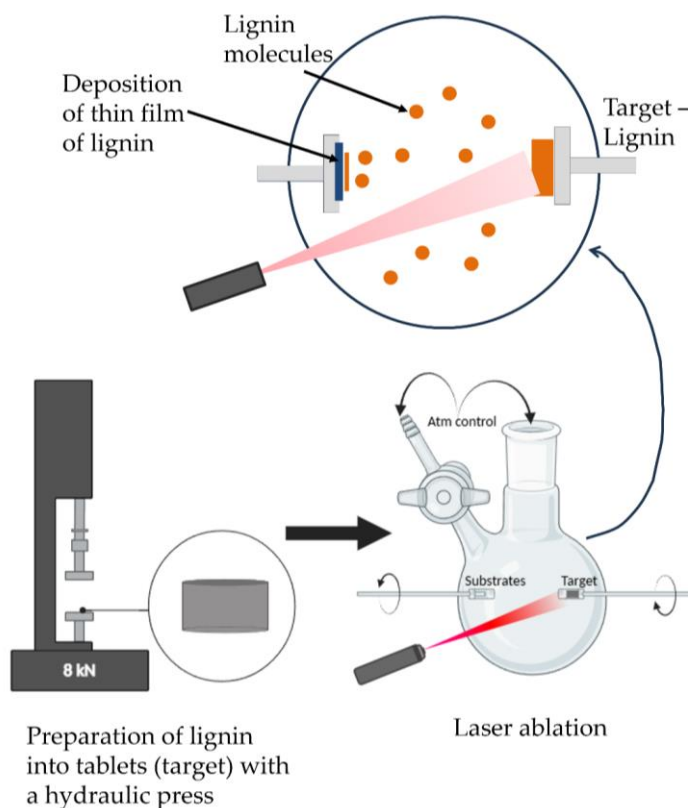


Figure 1.2. Schematic representation of the process of deposition of thin films by laser ablation.

2. Preparation of lignin/polymer composites by emulsion mixing

Introduction

Polymerization in an aqueous medium is an efficient and environmentally friendly alternative to traditional polymerization techniques. Water, as a continuous phase, not only contributes to greater safety during the synthesis, but also reduces the viscosity of the reaction medium. This improves heat transfer, allowing for more efficient control of temperature conditions, i.e. greater flexibility when preparing formulations. Compared to polymerization methods that use organic solvents, during polymerization in an aqueous medium, the emission of volatile organic components is significantly reduced, hence the ecological superiority of these systems (Pieters and Mekonnen, 2024; Prosheva et al., 2025).

Emulsion polymerization is most commonly used polymerization type for synthesis of aqueous polymer dispersions (Prosheva et al., 2025). Emulsion polymerization is a process of great industrial importance since it offers significant control over the morphology and structure of the polymer. Polymers that are

used as coatings, adhesives, paints, etc. are most commonly synthesized through emulsion polymerization (Cummings et al., 2019).

Emulsion polymerization is a heterogeneous free radical polymerization that consists of preparing a stable emulsion of hydrophobic monomers stabilized in an aqueous phase with the help of a surfactant. The conversion of monomers into polymer begins when an initiator is added to the system, which generates free radicals. After the reaction is complete, a stable dispersion of polymer particles in water is obtained, which is called a polymer dispersion or latex (Cummings et al., 2019).

In laboratory performed emulsion polymerization, several basic reactants are used: monomers, water, surfactant and initiator. In industrial conditions, emulsion polymerization formulations are much more complicated and can contain over 20 different components (Van Herk, 2013).

As already mentioned, water is used as a dispersion medium and this has several advantages, such as low viscosity and good heat transfer, but also low cost and reduced negative environmental impact (Berber, 2013). The monomers used in this process have reduced solubility in water, most often they are acrylate and methacrylate monomers, styrene, vinyl chloride and the like. Functional monomers are often added, these monomers are added in very small amounts and have some function, for example improving compatibility, improving crosslinking, reactivity, stability, etc. (Berber, 2013) In terms of initiators, initiators soluble in the aqueous phase (potassium, sodium and ammonium persulfates) and initiators soluble in the organic (monomer phase) (azobisbutyronitrile) are used. In certain cases, redox couple initiators can also be used. With regard to surfactants, several types can also be used, namely anionic, cationic, non-ionic or amphoteric (Van Herk, 2013).

The following text will briefly explain the mechanism of emulsion polymerization. Emulsion polymerization begins with the formation of micelles in the aqueous phase. Micelles are aggregates of surfactant and they form when the surfactant concentration reaches the critical micellar concentration, whereby a significant amount of surfactant remains dissolved in the aqueous phase. With the addition of monomers, a negligible amount dissolves in water, while the remainder of the monomer forms large monomer droplets stabilized by excess surfactant, and a portion of the monomers, about 1%, diffuses inside the micelles (Berber, 2013; Cummings et al., 2019; Lovell and Schork, 2020). Accordingly, before the initiator is added, an emulsion is formed consisting of three parts, an aqueous phase, large monomer droplets dispersed throughout the aqueous phase, and micelles containing dissolved monomers. The reaction begins with the addition of an initiator that dissociates into free radicals. The free radicals react with the monomers dissolved in water and form water-soluble oligomeric radicals. When these oligomers reach their critical length, they become hydrophobic and begin to enter the monomer-swollen micelles, resulting in the nucleation of a polymer particle (Cummings et al., 2019; Lovell and Schork, 2020). Since micelles have a larger specific surface area compared to monomer droplets, nucleation within micelles is the dominant mechanism; this type of nucleation is called micellar or heterogeneous and is dominant in cases where the surfactant concentration is above critical micellar concentration. Homogeneous nucleation occurs at lower surfactant concentrations. In this case, free radicals react with monomers stabilized in the aqueous phase to form oligomers. The oligomers are also stabilized by surfactant and they continue to grow in the aqueous phase, up to a certain critical degree of polymerization, after which the chains become insoluble in water and begin to precipitate (Cummings et al., 2019; Lovell and Schork, 2020).

Figure 2.1. shows the three intervals of emulsion polymerization.

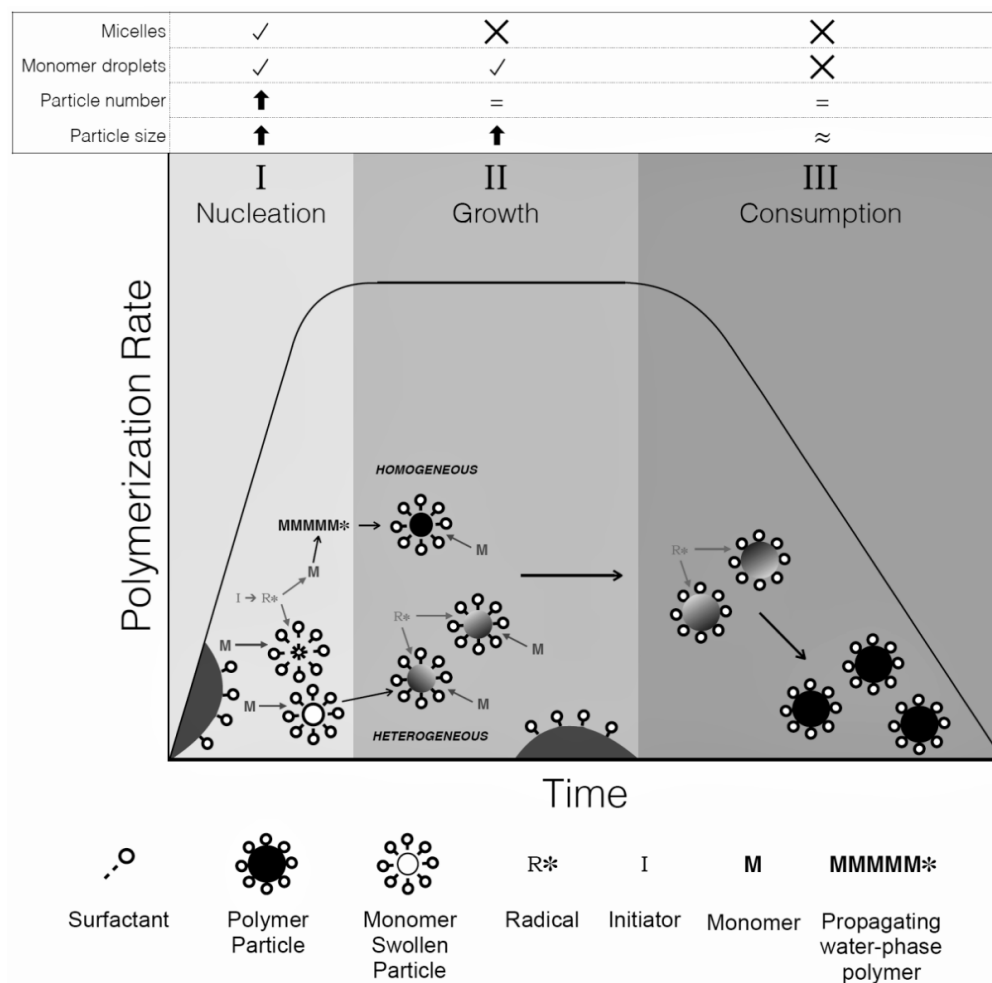


Figure 2.1. Schematic representation of the three intervals of emulsion polymerization (Cummings et al., 2019).

The first interval refers to the nucleation of polymer particles. In this interval the number of particles increases and thus the rate of polymerization increases with time. The monomer conversion at the end of this interval is below 20 wt% and this interval is considered to be complete when there are no monomer-swollen micelles in the system (Berber, 2013; Cummings et al., 2019). In the second interval, the polymerization rate is constant. During this interval, the diffusion of monomers from the monomer droplets to the growing polymer particles occurs, with the monomer concentration remaining constant in the polymer particles. Accordingly, the size of the polymer chains increases, and the monomer droplets decrease. The second interval is considered complete when the monomer droplets disappear. At the end of this interval, the monomer conversion is 50 to 80 wt%. In the third interval, the rate of polymerization begins to decrease, while the concentration of polymer in the formed particles increases until all the

monomer that has diffused into these particles is consumed. At the end of the reaction, an aqueous dispersion of polymer particles is obtained, which is called latex (Berber, 2013; Cummings et al., 2019). The morphology of the polymer, as well as its other properties, depend on the method of initiation, the reaction temperature, the added reagents, the presence of fillers, etc. (Cummings et al., 2019).

According to the size of the monomer droplets and the type of nucleation, emulsion polymerization is divided into three types. Conventional emulsion polymerization is also called macroemulsion polymerization. In this polymerization, the monomer droplets have dimensions from 1 to 100 μm and micellar nucleation (heterogeneous) occurs. Another type is microemulsion polymerization in which the monomer droplets have dimensions of 10 to 100 nm and micellar nucleation (heterogeneous) or homogeneous can occur depending on the amount of surfactant. The third type is miniemulsion, the monomer droplets in this polymerization have dimensions of 50 to 500 nm and homogeneous nucleation occurs (Berber, 2013).

A further division of emulsion polymerization can be made according to the degree of continuity of the process, i.e. a batch process, semi-continuous and continuous are distinguished. In the batch process, all reactants are mixed in a reactor, heated and after adding the initiator, polymerization begins. The semi-continuous process offers greater control over the polymerization reaction since some of the reactants (monomers, initiator, or water) are continuously added to the reaction system. In a continuous process, reactants are continuously added to the reaction system and product is simultaneously separated. The volume of reactants in the reactor remains constant (Berber, 2013).

The transition from latex to solid film occurs through three stages shown in Figure 2.2. The first stage consists of drying, or evaporation of water at a constant rate. With drying, the polymer chains begin to orient themselves. When the larger amount of water evaporates, the second stage, deformation, begins. During this period, the polymer chains are densely arranged next to each other and this occurs above the minimum film formation temperature (MFFT). First, a very thin film is formed on the surface and the remaining water evaporates by diffusion through this thin film. The polymer chains that are in contact with each other begin to deform. In the third stage, the polymer chains diffuse across the particle boundaries to reduce the surface energy, and the spheres coalesce into a continuous film (coalescence) (Cummings et al., 2019).

The production of composites by emulsion polymerization can be carried out through in-situ reaction or through emulsion mixing. In in-situ polymerization of a composite, the filler is added to the reactor along with the monomers and other reactants required for the reaction to proceed, with the conversion of the monomers into polymers taking place in the presence of the filler. This synthesis results in the formation of stable bonds between the filler and the polymer, such as hydrogen, polar, and in some cases covalent bonds (Prosheva et al., 2023). Emulsion mixing is a method that offers greater control over the characteristics of the polymer, given that the polymer matrix is synthesized first, and then the filler is incorporated with continuous mixing (Prosheva et al., 2025).

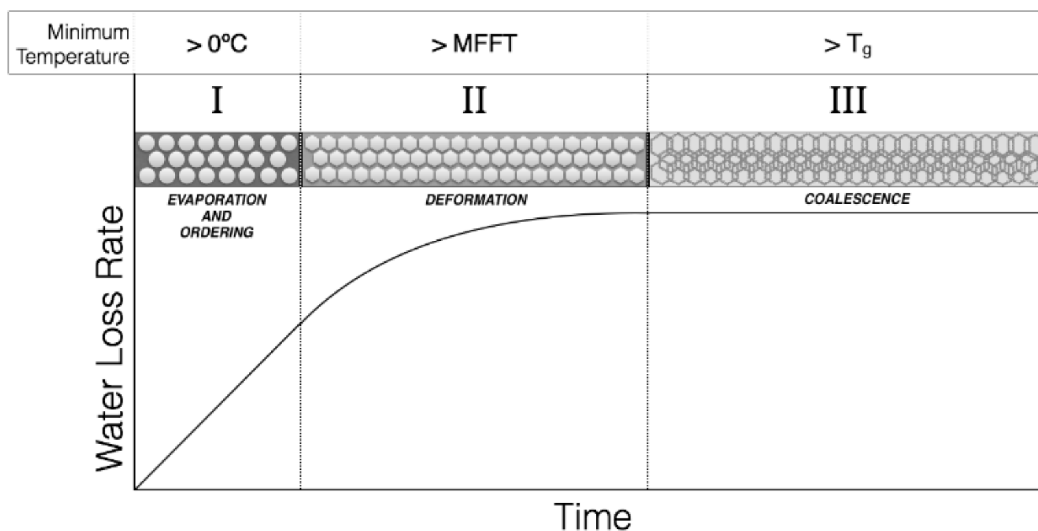


Figure 2.2. Schematic representation of the film formation mechanism (Cummings et al., 2019).

Experimental part

Purpose of the experiment

The aim of this experiment is to obtain lignin/polymer composites through emulsion mixing.

Equipment

Laboratory beakers
 Magnetic stirrer
 Tip-Sonicator
 Reactor
 Mechanical stirrer
 Water bath
 Condenser
 Thermometer
 pH meter
 Laboratory balance

Chemicals

Monomer – Butyl Acrylate (BA)
 Monomer – Methyl Methacrylate (MMA)
 Co-stabilizer – Octadecyl Acrylate (ODA)
 Surfactant – Dowfax 2A1 45% solution (alkyl diphenyl oxide disulfonate)
 Initiator – Potassium Persulfate (KPS)

Lignin
 0.1 M NaOH
 Deionized water

Performing the experiment

Polymer matrix synthesis

10 g of BA and 10 g of MMA are weighed into a beaker, 1.2 g of ODA are added to them, after which the reagents are mixed with a magnetic stirrer to dissolve the ODA (monomer phase). Meanwhile, 0.4 g of Dowfax and 75 g of deionized water are weighed into a separate beaker and mixed briefly (aqueous phase). Then the monomer and aqueous phases are mixed with a magnetic stirrer (200 rpm) and homogenized with a sonicator. Homogenization is performed with continuous stirring and in an ice bath. Sonication parameters are: 15 minutes effective time at 70% amplitude and 50% duty cycle. In this way a miniemulsion is obtained. The miniemulsion is then transferred to a reactor equipped with a mechanical stirrer, a thermometer and a nitrogen inlet. The reactor was heated using a water bath. When the temperature in the reactor reached 70°C, 0.1 g of KPS dissolved in 5 g of deionized water was added to the miniemulsion. The miniemulsion was then left to polymerize for 60 minutes at 70°C. The total water added should result in a polymer dispersion (latex) with a solids content of 20%. Figure 2.3. shows a schematic representation of the procedure for synthesizing a polymer matrix.

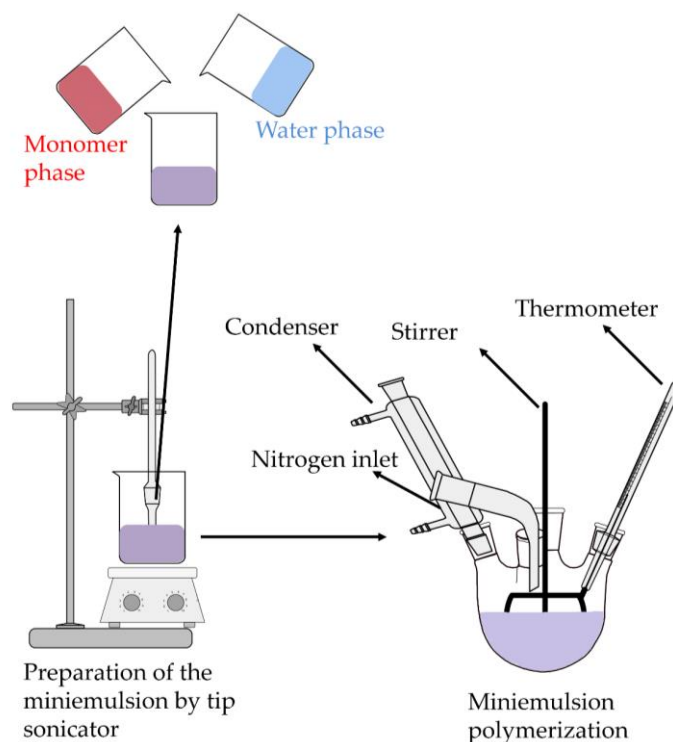


Figure 2.3. Miniemulsion polymerization.

Lignin dispersion

2 g of lignin and 50 g of deionized water were weighted into a beaker. While stirring continuously with a magnetic stirrer (200 rpm), 0.1 M NaOH was added until the pH reaches 10. The lignin dispersion was further homogenized with a tip-sonicator while stirring continuously and under the following conditions: 10 minutes effective time at 70% amplitude and 50% duty cycle.

Emulsion mixing

To obtain a lignin/polymer composite with 2 wt% lignin relative to polymer, 50 g of polymer dispersion is measured into a beaker. In another beaker, measure out 5.2 g of lignin dispersion. Add the lignin drop by drop to the polymer dispersion, while stirring continuously. After adding the lignin, the polymer dispersion, now a composite, is left to stir for another 10 minutes.

The dispersion is then poured into silicone molds and left to dry for five days at 23°C and 55% relative humidity. After drying, a solid film is obtained which is subjected to appropriate characterization. Figure 2.4 shows a schematic representation of the preparation of lignin/polymer composites by emulsion mixing.

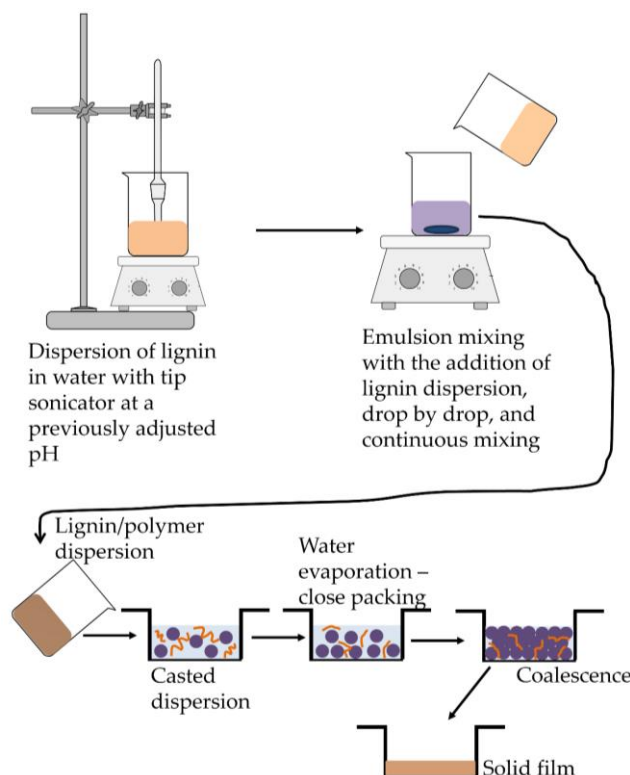


Figure 2.4. Preparation of lignin/polymer composites by emulsion mixing.

Interpretation of results

- Calculate the monomer conversion.

3. Characterization of Lignin/Polymer Composites

3.1 Fourier Transform Infrared Spectroscopy – FTIR

Introduction

Fourier Transform Infrared Spectroscopy – FTIR is a technique used to identify chemical bonds and functional groups in materials through the absorption of infrared (IR) light. When IR radiation passes through a sample, the molecules absorb energy at specific frequencies that correspond to their vibrations. The result of the measurement is a spectrum that shows the absorption as a function of frequency and serves as a “molecular fingerprint” of the sample.

FTIR spectrophotometer equipped with attenuating total reflection (FTIR-ATR) is based on a technique that allows analysis directly on the sample surface without special preparation (Liu and Kazarian, 2022; Tiernan et al., 2020). IR radiation is reflected from the surface through a crystal with a high refractive index, with a penetration depth of only a few micrometers (Tiernan et al., 2020). This makes ATR particularly suitable for examining thin layers, such as films or polymers, as well as for monitoring certain surface modifications. The obtained spectra can be easily compared with standard FTIR libraries for functional group identification, making the technique a fast and practical tool for controlling the quality and purity of materials, as well as for monitoring chemical reactions and structural changes.

Experimental part

Purpose of the experiment

Confirmation of the successful incorporation of lignin into the polymer matrix, by comparing the infrared spectra of lignin, polymer and lignin/polymer composite.

Equipment

FTIR spectrophotometer

Chemicals

Lignin

Polymer

Lignin/polymer composite

Performing the experiment

The characterization of the composite is performed with an FTIR spectrophotometer equipped with attenuated total reflection (ATR). The measurement is performed by placing the sample on the ATR crystal. The instrument is connected to appropriate software through which the parameters for performing the analysis are set. In addition to the spectrum of the lignin/polymer composite, spectra of

the lignin used to prepare the composite, as well as the polymer obtained according to the procedure described in **Polymer matrix synthesis**, are also recorded. The recorded spectra are processed in appropriate software.

Interpretation of results

- Compare the spectra of lignin, polymer and lignin/polymer composite.
- Using an appropriate database/literature, determine to which functional groups the characteristic spectral bands that appear in the spectra of lignin, polymer and lignin/polymer composite belong.
- Do new spectral bands appear in the lignin/polymer composite? Is the incorporation of lignin successful?

3.2 Contact angle measurement

Introduction

Contact angle is a term associated with the angle formed at the point of contact between a liquid, the solid surface on which the liquid is placed, and the ambient medium (gas), taking into account that the liquid is located on a horizontally placed solid surface. The interface formed between the three phases is also known as the “three-phase contact line” (Akbari and Antonini, 2021; Torbus et al., 2019). When measuring the contact angle, three possible cases are observed, as shown in Figure 3.1.

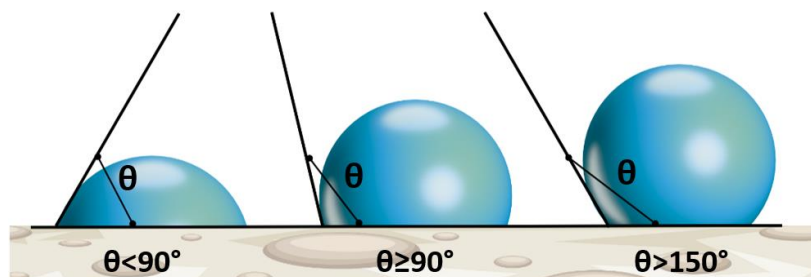


Figure 3.1. Illustration of contact angles formed by a liquid on a homogeneous solid surface.

It can be concluded that:

- 1) If the angle is less than 90°, the liquid spreads and the surface is well wetted.
- 2) If it is greater than 90°, the liquid remains in the form of a drop and the wetting is weak.
- 3) In superhydrophobic surfaces the angle is >150°, almost without contact with the surface ("lotus effect" – (Farzam et al., 2022)). The shape of the droplet that forms on the solid surface directly depends on the surface tension. The molecules inside the drop have reached equilibrium, but those on the surface are affected by neighboring molecules, creating internal pressure. Due to the appearance of internal pressure, the droplet tends to reduce its surface area in order to maintain a low free energy, which explains why droplets and bubbles assume a spherical shape (Torbus et al., 2019).

In reality, external forces (mainly gravity) deform the droplet, so the contact angle can be said to be the result of a combination of surface tension and external forces. From a theoretical point of view, it is characteristic of a particular liquid–solid system in a particular environment.

Experimental part

Purpose of the experiment

Study of the influence of lignin on the hydrophilicity/hydrophobicity of lignin/polymer composites by determining the water contact angle and comparing the contact angles of polymer and lignin/polymer composite.

Equipment

Contact angle measuring instrument with SEE System software

Chemicals

Polymer

Lignin/polymer composite

Deionized water

Performing the experiment

The sample is placed on the holder in front of the camera. Using a digital micropipette, 0.5 μl of deionized water is dropped onto the sample. The water drop is photographed and then analyzed with the appropriate SEE System software. The three-point method is used to determine the contact angle. Two points are placed on the liquid–solid interface in the drop image to define the substrate baseline, and the third point is placed on the drop contour (in the middle of the drop tip). After clicking on the third point, the contact angle is immediately calculated. Ten measurements are made for the polymer and the lignin/polymer composite, from which an average value is determined in order to achieve greater accuracy.

Interpretation of results

- What is the effect of lignin on the hydrophilicity/hydrophobicity of lignin/polymer composites? Why?

3.3 Tensile test

Introduction

Mechanical properties are part of the parameters that determine the use of materials. They describe the resistance to deformation (hardness, elasticity) and the ability to deform (plasticity). If the force is large

enough, it can also cause fracture in the tested materials, so it is important to know the relationship between force and deformation.

In polymers, the mechanical properties depend on the type of force, so tensile, compression and shear are distinguished, and certain more complex forces are also known, such as bending and torsion. Key parameters used to describe mechanical properties are:

- 1) Modulus of elasticity (E) – Young's modulus,
- 2) Tensile strength (σ_{\max}) – maximum stress before failure,
- 3) Yield strength (σ_y) – the point at which permanent deformation begins.

These properties and their development are given by the stress-strain curve, which is most often obtained by an elongation test. A standard sample, called a test piece (in the shape of a "dog bone"), is stretched to failure, and the results are measured with a tensile test instrument equipped with extensometer that registers the force and elongation. The test piece, whose dimensions are prescribed by a standard (must be specified because they directly affect the results, (G. Zhang et al., 2023)), is clamped appropriately within the instrument and elongated at a constant speed. During the stretching, the so-called extensometer monitors the elongation, as well as the applied force for it.

To eliminate the influence of geometry, normalized parameters are used (Faridmehr et al., 2014):

- 1) Engineering stress: $\sigma = F/A_0$ (N/m² or MPa),
- 2) Engineering strain: $\varepsilon = (L - L_0)/L_0$ (dimensionless or in %).

The ratio of these two parameters, stress and strain, gives the modulus of elasticity (E).

Experimental part

Purpose of the experiment

Study of the influence of lignin on the mechanical properties of lignin/polymer composites through elongation testing and comparison of mechanical properties between polymer and lignin/polymer composite.

Equipment

Shimadzu universal instrument for testing mechanical properties

Hydraulic press

Calliper

Chemicals

Polymer

Lignin/polymer composite

Performing the experiment

Before starting the measurement, the polymer and lignin/polymer composite are cut into samples of appropriate shape and dimensions using a hydraulic press. The universal instrument for testing

mechanical properties is connected to appropriate software through which data relating to the thickness, width and length of the sample are entered. Data on the conditions under which the measurement is performed, such as the elongation rate, are also entered. The sample is placed on the appropriate holders, the extensometer is also fixed, after which the measurement can begin.

Interpretation of results

- Using appropriate software, plot a stress-strain graph and read the data related to the modulus of elasticity, tensile strength, yield strength, and elongation.
- Compare the graph and the data of the polymer and the lignin/polymer composite.
- How does the incorporation of lignin affect the mechanical behavior of the resulting composite?

References:

Akbari, R., Antonini, C. (2021). Contact angle measurements: From existing methods to an open-source tool. *Adv. Colloid Interface Sci.* 294, 102470. <https://doi.org/10.1016/j.cis.2021.102470>.

Berber, H. (2013). Emulsion Polymerization: Effects of Polymerization Variables on the Properties of Vinyl Acetate Based Emulsion Polymers, in: Yilmaz, F. (Ed.), *Polymer Science*. InTech, Rijeka. <https://doi.org/10.5772/51498>.

Claverie, F. (2020). Laser ablation, in: Beauchemin, D. (Ed.), *Sample Introduction Systems in ICPMS and ICPOES*. Elsevier, Amsterdam, pp. 469–531. <https://doi.org/10.1016/B978-0-444-59482-2.00010-5>.

Cummings, S., Zhang, Y., Smeets, N., Cunningham, M., Dubé, M.A. (2019). On the use of starch in emulsion polymerizations. *Processes* 7, 140. <https://doi.org/10.3390/pr7030140>.

Faridmehr, I., Osman, M.H., Adnan, A.B., Nejad, A.F., Hodjati, R., Azimi, M.A. (2014). Correlation between Engineering Stress-Strain and True Stress-Strain Curve. *Am. J. Civ. Eng. Archit.* 2, 53–59. <https://doi.org/10.12691/ajcea-2-1-6>.

Farzam, M., Beitollahpoor, M., Solomon, S.E., Ashbaugh, H.S., Pesika, N.S. (2022). Advances in the fabrication and characterization of superhydrophobic surfaces inspired by the lotus leaf. *Biomimetics* 7, 196. <https://doi.org/10.3390/biomimetics7040196>.

Liu, G.L., Kazarian, S.G. (2022). Recent advances and applications to cultural heritage using ATR-FTIR spectroscopy and ATR-FTIR spectroscopic imaging. *Analyst* 147, 1777–1797. <https://doi.org/10.1039/d2an00005a>.

Lovell, P.A., Schork, F.J. (2020). Fundamentals of emulsion polymerization. *Biomacromolecules* 21, 4396–4441. <https://doi.org/10.1021/acs.biomac.0c00769>.

Pieters, K., Mekonnen, T.H. (2024). Progress in waterborne polymer dispersions for coating applications: commercialized systems and new trends. *RSC Sustain.* 2, 3704–3729. <https://doi.org/10.1039/d4su00267a>.

Prosheva, M., Ehsani, M., Joseph, Y., Tomovska, R., Blazhevskia Gilev, J. (2023). Waterborne polymer composites containing hybrid graphene/carbon nanotube filler: Effect of graphene type on properties and performance. *Polym. Compos.* 44, 5188–5200. <https://doi.org/10.1002/pc.27483>.

Prosheva, M., Ozmen-Monkul, B., Gumus, G., Taskin, D.K., Trajcheva, A., Blazevska-Gilev, J., Tomovska, R. (2025). Waterborne advanced optical coatings based on polymer composite with hybrid graphene–metal phthalocyanine nanofiller. *Prog. Org. Coat.* 204, 109260. <https://doi.org/10.1016/j.porgcoat.2025.109260>.

Ravi-Kumar, S., Lies, B., Lyu, H., Qin, H. (2019). Laser ablation of polymers: A review. *Procedia Manuf.* 34, 316–327. <https://doi.org/10.1016/j.promfg.2019.06.155>.

Russo, R.E., Mao, X.L., Yoo, J.H., Gonzalez, J.J. (2007). Laser ablation, in: Singh, J.P., Thakur, S.N. (Eds.), *Laser-Induced Breakdown Spectroscopy*, second ed. Elsevier, Amsterdam, pp. 41–70. ISBN 978-0-12-818829-3.

Tiernan, H., Byrne, B., Kazarian, S.G. (2020). ATR-FTIR spectroscopy and spectroscopic imaging for the analysis of biopharmaceuticals. *Spectrochim. Acta A Mol. Biomol. Spectrosc.* 241, 118636. <https://doi.org/10.1016/j.saa.2020.118636>.

Torbus, S., Dolata, M., Jakiela, S., Michalski, J.A. (2019). Analysis of existing thermodynamic models of the liquid drop deposited on the substrate – a sufficient condition of the minimum free energy of the system. *Coatings* 9, 791. <https://doi.org/10.3390/coatings9120791>.

Van Herk, A.M. (2013). *Chemistry and Technology of Emulsion Polymerisation*, 2nd ed. Wiley-Blackwell, Oxford. ISBN 978-1-118-63836-1.

Zhang, D., and Guan, L. (2014). Laser Ablation. In *Comprehensive Materials Processing: Thirteen Volume Set* (Vol. 4, pp. V4-125-V4-169). Elsevier. <https://doi.org/10.1016/B978-0-08-096532-1.00406-4>.

Zhang, G., Wang, Q., Ni, Y., Liu, P., Liu, F., Leguillon, D., Xu, L.R. (2023). A systematic investigation on the minimum tensile strengths and size effects of 3D printing polymers. *Polym. Test.* 117, 107845. <https://doi.org/10.1016/j.polymertesting.2022.107845>.